Efficacy of the Immobilized *Kocuria flava* Lipase on Fe₃O₄/Cellulose Nanocomposite for Biodiesel Production from Cooking Oil Wastes

Azhar A. Najjar [1], Elhagag A. Hassan [2,*], Nidal M. Zabermawi [1], Saad B. Almasaudi [1], Mohammed Moulay [1,3], Steve Harakeh [4,5,*] and Mohamed Abd El-Aal [6,*]

[1] Department of Biological Sciences and Microbiology, Faculty of Science, King Abdulaziz University, Jeddah 21589, Saudi Arabia

[2] Department of Botany and Microbiology, Faculty of Science, Assiut University, Assiut 71516, Egypt

[3] Vaccines and Immunotherapy Unit, King Fahd Medical Research Center, King Abdulaziz University, Jeddah 21589, Saudi Arabia

[4] King Fahd Medical Research Center, King Abdulaziz University, Jeddah 21589, Saudi Arabia

[5] Yousef Abdul Lateef Jameel Chair of Prophetic Medicine Application, Faculty of Medicine, King Abdulaziz University, Jeddah 21589, Saudi Arabia

[6] Catalysis and Surface Chemistry Laboratory, Chemistry Department, Faculty of Science, Assiut University, Assiut 71516, Egypt

[*] Correspondence: elhagaghassan@aun.edu.eg (E.A.H.); sharakeh@gmail.com (S.H.); mohamedabdelaal@aun.edu.eg (M.A.E.-A.)

Abstract: The increasing global demand for petroleum oils has led to a significant increase in their cost and has led to the search for renewable alternative waste resources for biodiesel synthesis and production using novel environmentally sound and acceptable methods. In the current study, *Kocuria flava* lipase was immobilized on Fe₃O₄/cellulose nanocomposite; and used as a biocatalyst for the conversion of cooking oil wastes into biodiesel through the transesterification/esterification process. The characterization of Fe₃O₄/cellulose nanocomposite revealed several functional groups including carboxyl (C=O) and epoxy (C-O-C) groups that act as multipoint covalent binding sites between the lipase and the Fe₃O₄/cellulose nanocomposite and consequently increasing lipase immobility and stability. The immobilized lipase showed a high thermo-stability as it retained about 70% of its activity at 80 °C after 30 min. The kinetics of immobilized lipase revealed that the K_m and V_{max} values were 0.02 mM and 32.47 U/mg protein, respectively. Moreover, the immobilized lipase showed high stability and reusability for transesterification/esterification reactions for up to four cycles with a slight decline in the enzyme activity. Furthermore, the produced biodiesel characteristics were compatible with the standards, indicating that the biodiesel obtained is doable and may be utilized in our daily life as a diesel fuel.

Keywords: Fe₃O₄/cellulose nanocomposite; biocatalyst; biodiesel; transesterification/esterification process; *Kocuria flava* lipase; immobilized lipase

1. Introduction

The world's strategic petroleum reserves will eventually run out due to higher demand for development, transportation, and industrialization [1,2]. This is in addition to certain political unrest and wars which resulted in certain restrictions and higher costs. There are also many environmental issues that are involved including environmental pollution. For this reason, the search for an alternative has been sought. One of these alternatives includes the use of prospective sustainable alternative energy sources for bioenergy generation [3,4]. Biodiesel is one of the most prevalent prospective renewable resources that is produced from oil/fat feed-stocks biomass through transesterification/esterification processes through chemical or enzymatic reactions [5]. Enzymatic catalysis enables the

use of low-quality inedible oil and waste cooking oil [6], thereby reducing environmental issues and costs associated with subsequent production processes [7]. It also allows for milder production conditions (temperature, pH, and pressure) with lower amounts of by-products. Enzymatic transesterification/esterification reactions are considered greener than chemical processes and have recently attracted a great deal of attention. Such processes involve the use of an effective and recyclable biocatalyst instead of conventional catalysts due to the growing environmental issues associated with their use [5]. Consequently, a significant increase in developing newer and novel technologies for biodiesel production has been evident. However, there are some issues with enzyme recovery and recycling that make the lipase-mediated industrial transesterification processes less effective [8,9]. Numerous research efforts have been made to immobilize lipases on suitable carriers for the improvement of lipase enzyme activities in an effort to overcome these challenges. However, several lipase immobilization strategies have intensively been exploited for the enzymatic transesterification process [10,11]. There are many drawbacks concerning the carrier material to be used which showed a significant impact on the performance and activities of the immobilized lipases. Therefore, the use of biological nanocomposites can retain high amounts of lipases with superior activities [12], due to the greater surface/volume ratio as well as less mass dispersal restriction [13]. However, certain drawbacks have been noted and some of these include (1) the recovery of the nanocomposite carriers by filtration or centrifugation is extremely difficult, (2) loss of the biocatalyst activity, and (3) higher energy consumption is needed [12,14]. To enhance the application and feasibility of nanocomposite carriers alternative recovery methods are required for simple enzyme recovery. Interestingly, magnetic nanoparticles can be used for enzyme support because of their easy recovery using an external magnetic field with negligible biocatalyst loss [15–17]. Immobilization of biological nanocomposite with magnetic nanoparticles may be considered a potential and attractive way for increasing lipase enzyme activity and recyclability as well as the stability of the magnetic nanoparticles [18–20].

Magnetic nanoparticles (NPs) are essential not only in the study of catalysis [21], but also in a variety of other areas of research, including material science, advanced technological and medicinal applications, and green chemistry [22–26]. Magnetic NPs play an essential role in the conversion of vegetable oils into biodiesel, with two primary advantages [27]. The nanoscale particles enhance the surface area of the catalyst, thereby increasing its activity status, and it may also be easily separated from biodiesel and crude with a high recovery rate using an external magnetic field [28]. Among all the magnetic nanomaterials, Iron-based nanoparticles are of great interest due to their favorable magnetic and electrical properties. They are mainly divided into three types i.e., α-Fe_2O_3, γ-Fe_2O_3 [29], and Fe_3O_4 [30]. Among them, Fe_3O_4 is non-toxic, easily prepared, and has the largest saturation magnetization. Fe_3O_4 NPs properties are highly dependent on their shape, size, and surface chemistry, so accurate control over the nanoparticle synthesis process is essential. Several chemical, physical, and biological methods are used for their synthesis [31]. However, an unmodified catalyst is reversible, and the reaction is unstable because it can easily be agglomerated and oxidized due to the presence of Fe^{2+} [23]. Therefore, it is essential to develop nanocomposite material using a support that can protect Fe_3O_4 NPs.

Nano-cellulose is a carbohydrate polymer that functions as a sustainable nanomaterial due to its biodegradability, biocompatibility, and porous nature. It has the potential to be employed as an effective support material since it can form bonds with a variety of functional groups, for example, it was used as a supporting material for Fe_3O_4 in the synthesis of biodiesel from oleic acid [32].

Based on the increasing interest in biotechnological applications of microbial lipases for producing biodiesel using lipase transesterification and esterification techniques from used cooking oil, this study was conducted with the objectives to enhance bioenergy production technology via the improvement of the lipase transesterification/esterification activity with the aim to develop lipase immobilization process with coupled nanocomposites of

biological (nanocellulose) and magnetic nanoparticles. In addition, characterizing the immobilized lipase using different techniques and its activity and kinetics was evaluated. Furthermore, the reusability of immobilized lipase for transesterification/esterification was checked and the characteristics of the produced biodiesel were compared to conventional standard products.

2. Results

2.1. Production and Purification of Kocuria flava ASU5 Lipase

Kocuria flava MT919305 lipase purification process was performed using salt precipitation process, followed by the dialysis separation to get a partially purified enzyme. The activity of the bacterial lipase varied with different enzymatic conditions, while the lipase crude enzyme activity exhibited 15.03 ± 0.62 U/mL and that of the partially purified enzyme was 25.24 ± 2.03 U/mL. The specific activities of the crude enzyme and the partially purified enzyme were 33.35 ± 1.94 and 38.83 ± 2.07 U/mg protein, respectively (Table 1). Consequently, the partially purified enzyme was used for immobilization and encapsulation using the prepared nanomaterials. Furthermore, the activity of the biocatalyst was determined under different reaction conditions.

Table 1. Activity, protein content, and lipases specific activity of crude and partially purified enzyme.

	Activity (U/mL)	Protein Content (mg/mL)	Specific Activity U/mg Protein
Crude enzyme	15.03 ± 0.62	0.45 ± 0.32	33.35 ± 1.94
Partially purified enzyme	25.24 ± 2.03	0.65 ± 0.98	38.83 ± 2.07

2.2. Synthesis and Characterization of Nanocomposite and Immobilization of Kocuria flava ASU5 Lipases

The FTIR spectra of Fe_3O_4 NPs, nanocellulose, Fe_3O_4/cellulose nanocomposite, and Fe_3O_4/nanocellulose/lipase enzyme are displayed in Figure 1. For the Fe_3O_4 NPs, there are various function groups were recorded at 3424 cm^{-1}, 2921 cm^{-1}, 2850 cm^{-1}, 1628 cm^{-1}, 634 cm^{-1}, 560 cm^{-1}, and 445 cm^{-1}. For the nanocellulose, the characteristic bands were assigned as follows: 3416 cm^{-1}, 2901 cm^{-1}, 1640 cm^{-1}, 1570 cm^{-1}, 1431 cm^{-1}, 1373 cm^{-1}, 1164 cm^{-1}, 1113 cm^{-1}, 1060 cm^{-1}, 1033 cm^{-1}, 902 cm^{-1}, 670 cm^{-1}, and 615 cm^{-1}. The other characteristic bands of pure nanocellulose were the same as Fe_3O_4/nanocellulose and Fe_3O_4/nanocellulose/lipase enzyme. No characteristic bands of Fe_3O_4 NPs or lipase enzyme could be detected. Data in Figure 2 shows the TEM images of Fe_3O_4 NPs, nanocellulose, and Fe_3O_4/nanocellulose nanocomposite. It was observed that the prepared Fe_3O_4 has a spherical shape with an average particle size of ~34.5 nm. The nanocellulose (Figure 2b) showed a fiber structure with an average width of ~49 nm and an average length of ~526 nm. On the other hand, the micrograph of the Fe_3O_4/nanocellulose nanocomposite (Figure 2c) showed small dark-colored spherical particles and a fiber-like structure (lighter in color).

2.3. Characterization of Partially Purified Free Kocuria flava ASU5 Lipase and Immobilized Lipases

Lipase enzymes are primarily responsible for catalyzing the conversion of triglycerides into fatty acids and glycerol. As interfacial enzymes, lipases need an interface to carry out their catalytic activities. This is due to the fact that their physiological medium is aqueous while their substrate (triglycerides) is insoluble in water [33]. Lipase thus operates at the water/oil interface. When the substrate concentration is high enough to generate micellar solutions or emulsions, or interfaces, the activity of lipases is greatly improved. Lipases have relatively lower activity toward molecularly dispersed substrates in aqueous solution. The reaction mixture's conditions and the carrier's hydrophobicity were the key factors affecting lipase activity. More hydrophobic carriers than less hydrophobic ones enhanced lipase activity [33].
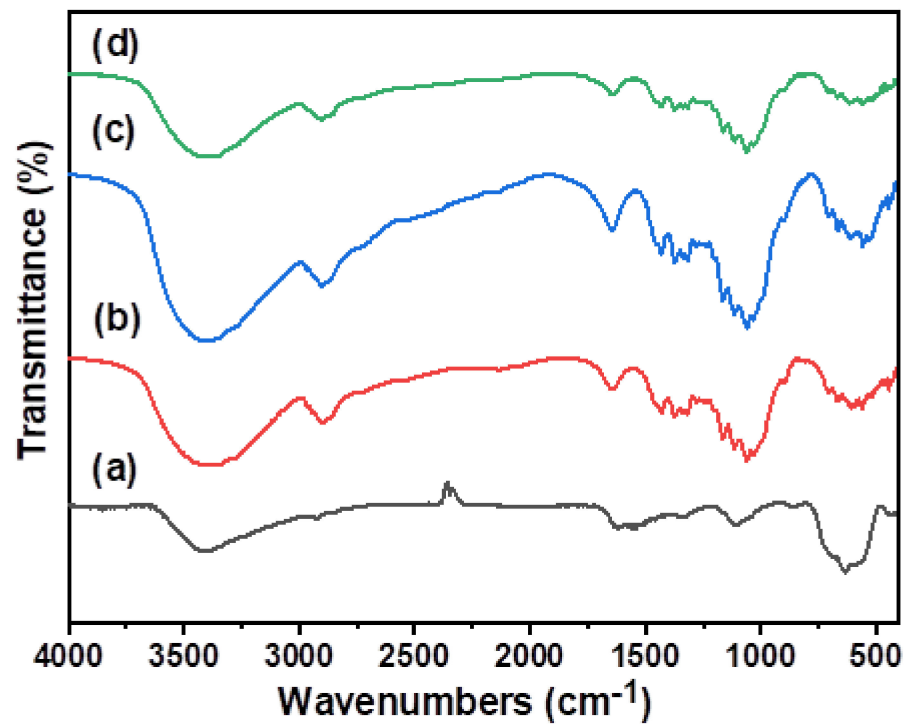
Figure 1. FTIR spectra of (**a**) Fe_3O_4 NPs, (**b**) nanocellulose, (**c**) Fe_3O_4/cellulose nanocomposite, and (**d**) Fe_3O_4/ nanocellulose/lipase enzyme composite.
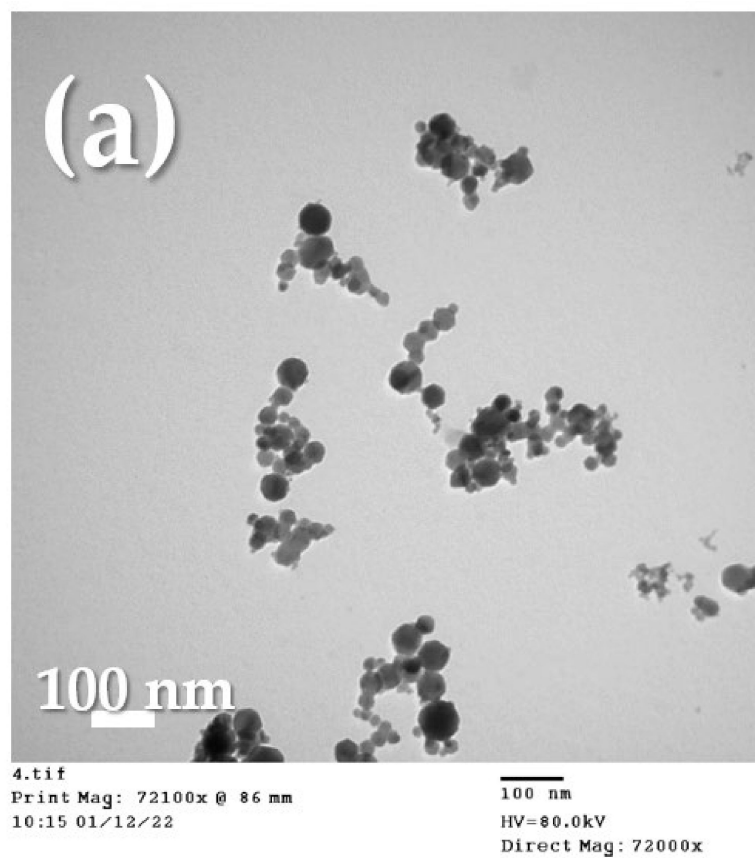
Figure 2. *Cont.*
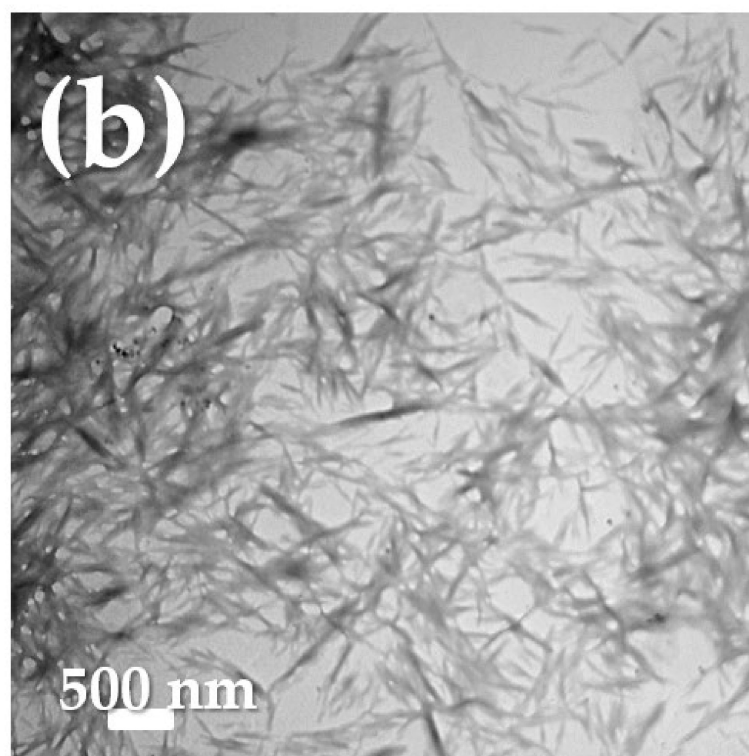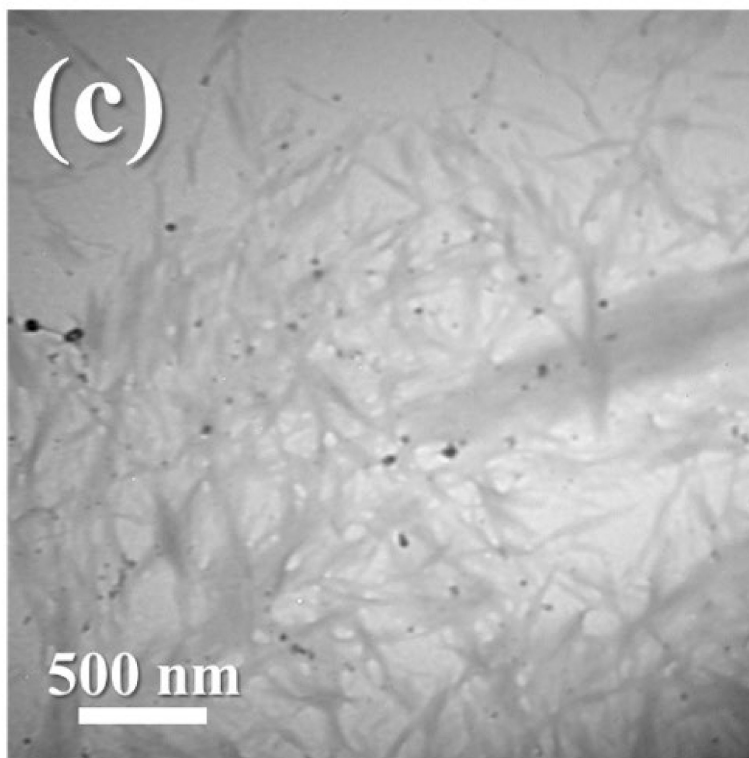
Figure 2. TEM images of (**a**) Fe_3O_4 NPs, (**b**) nanocellulose, and (**c**) Fe_3O_4/cellulose nanocomposite.

2.3.1. Effect of Reaction Temperature

The effect of reaction temperature on the partially purified free enzyme and nanocompo site-lipase specific activities was investigated at different incubation temperatures (40, 45, 50, 55, 60, 65, and 70 °C). The results showed that the specific activities of the tested lipases increased between 40 °C to 55 °C for partially purified free lipase at temperatures between 40 °C to 60 °C in the case of the immobilized bacterial lipase. The optimum temperature for the partially purified free lipase activity was 55 °C recording 34.05 U/mg protein (Figure 3) and the optimum incubation temperature for the immobilized lipase was 60 °C recording 36.97 U/mg protein. After that, an insignificant reduction in the lipase-specific activities was noted above the optimum temperatures for both partially purified free and immobilized lipases. At an incubation temperature of 65 °C, there was a significant reduction in the partially purified free lipase specific activities down to 33.22% as compared to that at optimum temperature. The specific activity of the immobilized lipase enzyme at the incubation temperature of 70 °C revealed a reduction of the activity by 44.20% (Figure 3).
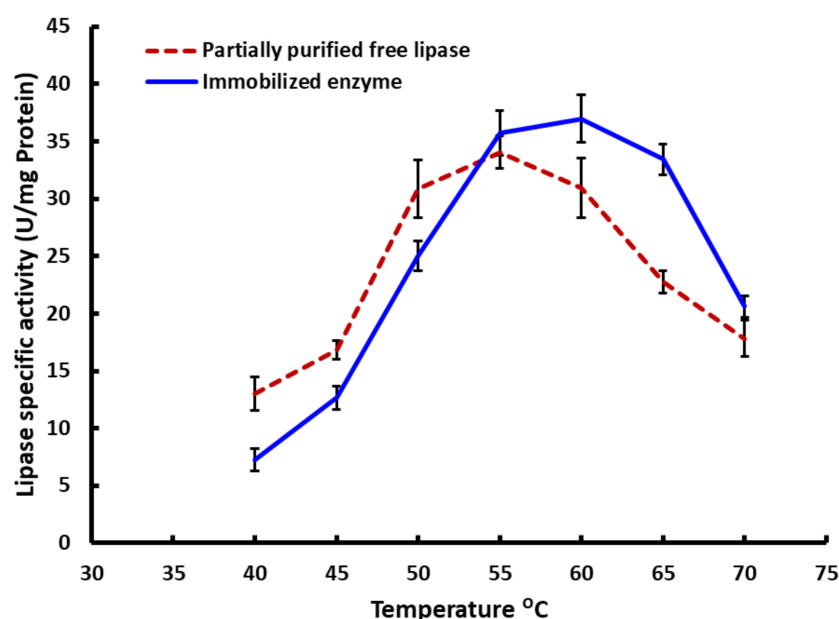

Figure 3. Effect of the reaction mixture temperature on the partially purified free enzyme and immobilized lipase-specific activities. The means value of three replicates ±SD (vertical bars) is represented.

2.3.2. Effect of Hydrogen Ion Concentration

The effect of pH (3, 4, 5, 6, 7, 8, and 9) was evaluated on both partially purified free *Kocuria flava* lipase enzyme and its immobilized lipase-specific activity. The results indicated that the lipase activity increased with increasing the pH value, with an optimum pH value of ~8 (Table 2). However, the partially purified free lipase activity declined dramatically at pH 9 as compared to the immobilized lipase.

Table 2. Effect of pH concentration of the reaction mixture on the partially purified free enzyme and immobilized lipase-specific activities. The means value of three replicates ± SD is represented.

pH	Enzyme Specific Activity (U/mg Protein)	
	Partially Purified Free Lipase	**Immobilized Enzyme**
4	11.49 ± 1.96	9.04 ± 0.45
5	21.73 ± 1.83	20.32 ± 1.13
6	26.49 ± 4.01	27.93 ± 0.55
7	30.26 ± 1.85	34.87 ± 0.45
8	35.87 ± 2.25	39.7 ± 1.4
9	20.71 ± 0.43	32.53 ± 0.97

2.3.3. Assay of Thermo-Stability

The thermo-stability of the partially purified free and the immobilized lipase were assayed at different time intervals (5–120 min) and at different reaction temperatures (50, 60, 70, 80, and 90 °C). The data revealed that the activities of the partially purified free lipases retained 90% of their activity at 50 °C and for 15 min of exposure. This was followed by a significant decline in their activity with increasing the reaction temperature. A faster activity drop was observed in the case of partially purified free lipase enzyme with increasing the reaction temperature (Figure 4a). In comparison to the partially purified free lipase, the immobilized lipase could sustain its greater specific activity at a higher reaction temperature (Figure 4b). The immobilized lipase activity continued to be active at a reaction temperature of 80 °C for 30 min. However, the free lipase was significantly deactivated at reaction temperatures higher than 80 °C as shown in Figure 4.
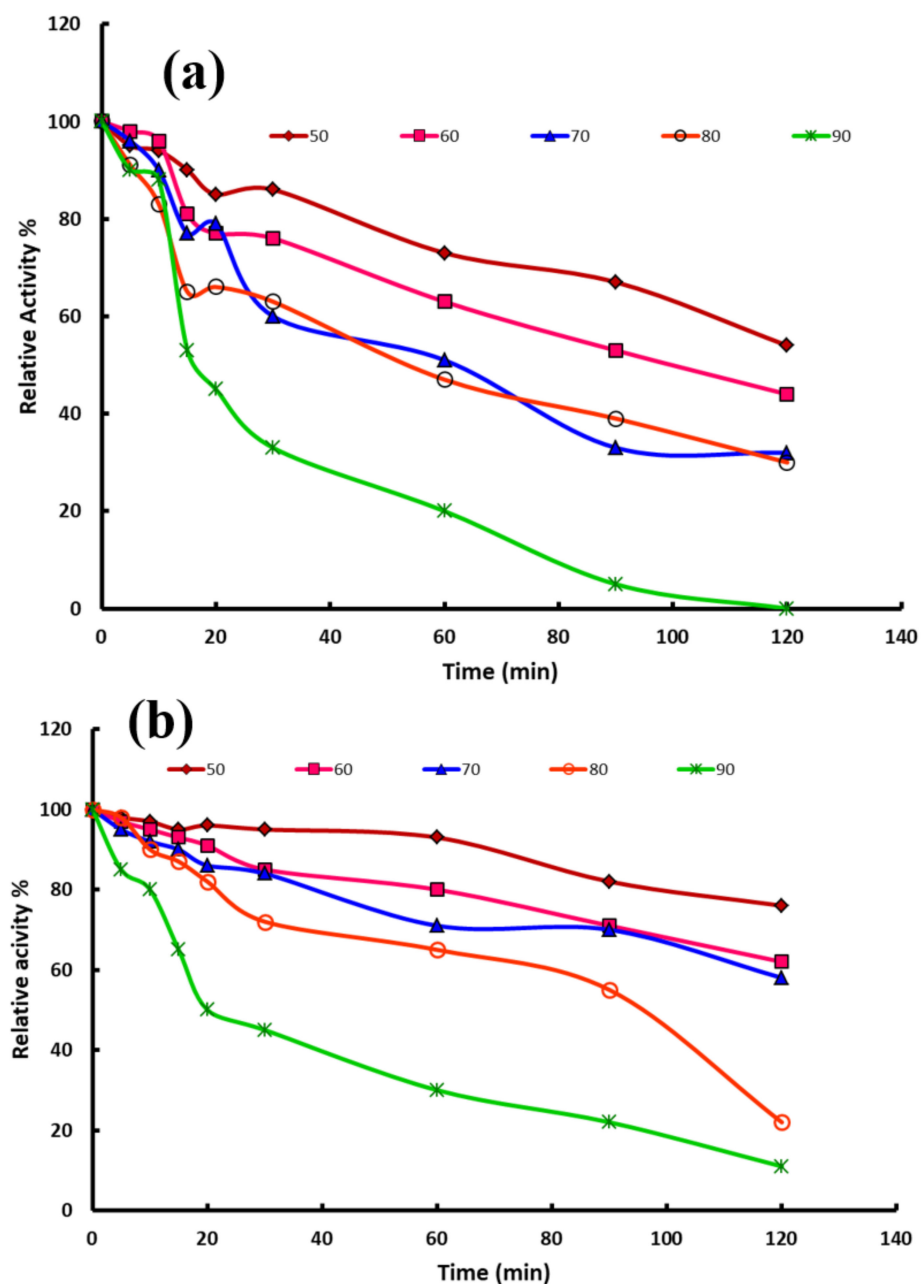

Figure 4. Thermo-stability of the partially purified free enzyme (**a**) and immobilized lipase (**b**).

2.4. Kinetics of the Immobilized Lipase Enzyme

The kinetic parameters of the immobilized lipase enzyme K_m and V_{max} values were estimated using Lineweaver-Burk plot (Figure 5). The K_m and V_{max} values for the *Kocuria flava* ASU5 immobilized lipase were approximately 0.02 mM and 32.47 U/mg protein, respectively.
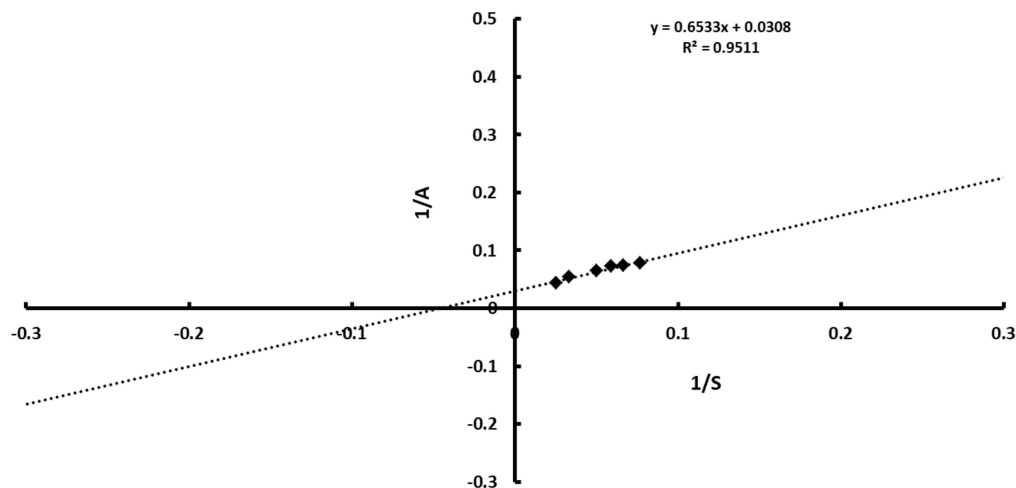

Figure 5. Lineweaver-Burk plot plots for *Kocuria flava* ASU5 immobilized lipase.

2.5. The Efficiency of Biodiesel Synthesis and the Reusability of the Immobilized Lipase

Data obtained by GC/MS analysis revealed that the most common fatty acid methyl ester detected after the transesterification process were 9-octadecenoic acid, hexadecanoic acid, octadecanoic acid, heptanoic acid, 9,12-octadecadienoic acid and 9,10-epoxy-octadecanoic acid methyl esters recording 27.14%, 19.2%, 8.47%, 5.99%, 3.24% and 2.65% of the total analytes, respectively. Other fatty acid methyl esters were detected using GC/MS analysis as shown in Figure 6. Biodiesel yield from the transesterification process of the waste cooking oils with the immobilized enzyme was 91.07% at a reaction temperature of 60 °C and incubation period of 5 h. The immobilized lipase maintained its activity in the recycle assay and could be treated four times with slightly observable activity loss, yielding 74.53% fatty acid methyl esters (FAMEs) (Figure 7).
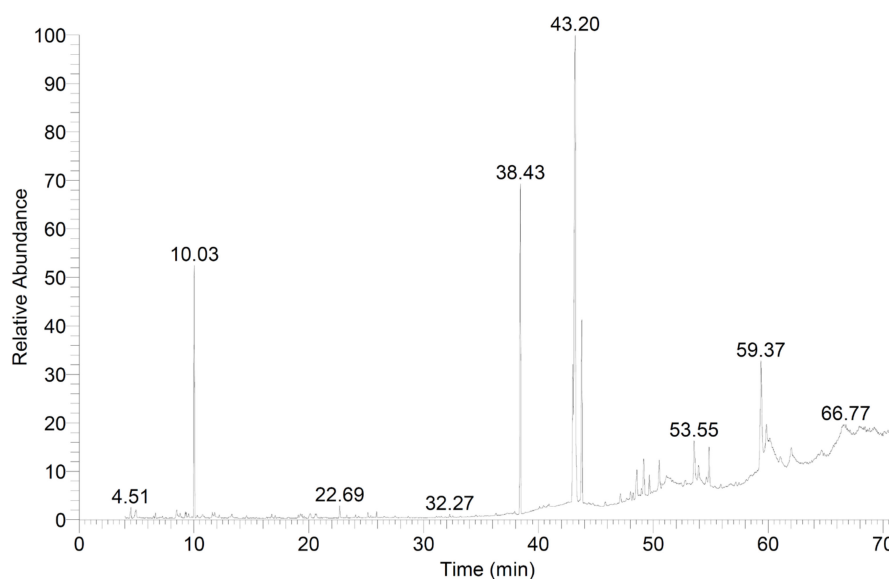

Figure 6. GC/MS graph for biodiesel analysis produced from transesterification/esterification process of waste cooking oils by immobilized lipase.
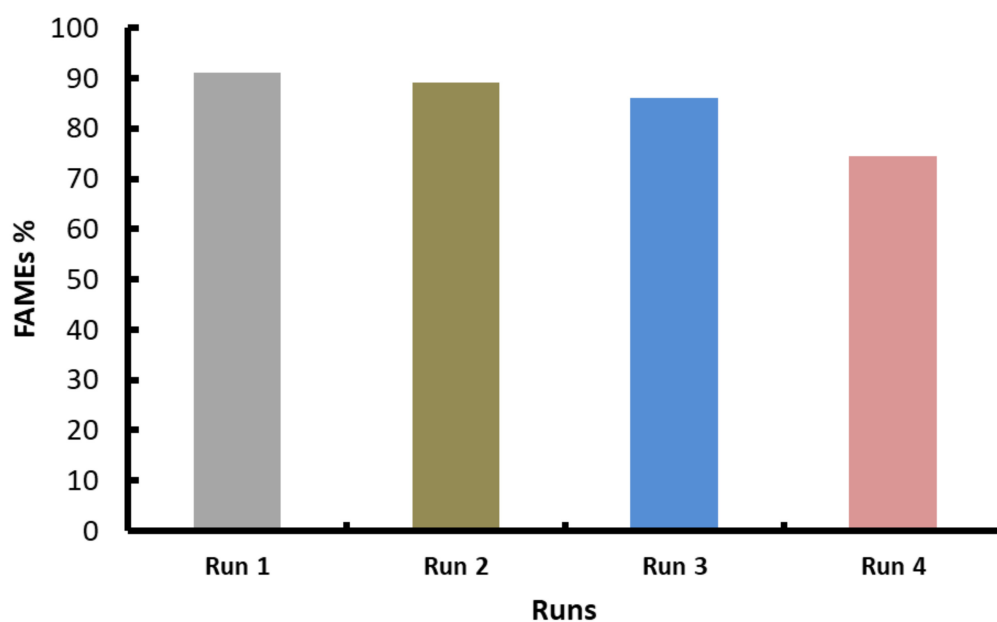
Figure 7. The reusability of *Kocuria flava* ASU5 immobilized lipase for biodiesel synthesis.

2.6. Properties of Obtained Biodiesel from Immobilized Lipase Transesterification/Esterification Process

The physicochemical properties of the produced biodiesel from the transesterification process of cooking oil wastes were calculated mathematically from the provided equations using GC/MS analysis (Figure 6). The following characteristics of the biodiesel produced included: determination of biodiesel density (ρ), kinematic viscosity (ν_{mix}), saponification number (SN), iodine value (IV), higher heating value (HHV), Cetane Number (CN), and free fatty acid (FFA) of the produced biodiesel and concentration of linolenic acid (C18:2) (%) were 0.64 g.cm^{-3}, 3.6 mm^2 s^{-1}, 128.69, 33.74, 43.65 MJ kg^{-1}, 59.02, 5.98% and 3.24%, respectively. In addition, FAME having ≥ 4 double bonds were not detected in the transesterified cooking oil wastes by lipase transesterification/esterification process (Table 3).

Table 3. Properties of fatty acid methyl esters produced by immobilized lipases transesterification process.

Property	Value	Standard	
		US Biodiesel Standard ASTM D6751	**EU Biodiesel Standard EN 14214**
Density (g.cm^{-3})	0.642	NS	0.86–0.90
Kinematic viscosity (40 °C; mm^2 s^{-1})	3.6	1.9–6.0	3.5–5.0
SN	128.69	NS	NS
IV	33.74	NS	120 max
HHV (MJ kg^{-1})	43.65	NS	NS
CN	59.02	47–65	51 min
FFA (%)	5.98	NS	NS
Concentration of linolenic acid (C18:2) (%)	3.24	NS	12 max
FAME having ≥ 4 double bonds (%)	ND	NS	1 max

3. Discussion

3.1. Production and Purification of Kocuria flava ASU5 Lipase

The obtained data revealed that the activity of the bacterial lipase varied with further purification processes. The crude lipase exhibited enzyme activity of 15.03 $\pm$ 0.62 U/mL and specific activities of 33.35 $\pm$ 1.94 U/mg protein, whereas the lipase activity and specific activity of the partially purified enzyme were 25.24 $\pm$ 2.03 U/mL and 38. 83 $\pm$ 2.07 U/mg protein, respectively. Najjar et al. [34] reported that the *Kocuria fava* MT919305 lipases

showed promising thermostable and methanol-tolerant properties, which may increase enzyme economic feasibility for the synthesis of green energy. Furthermore, the *Kocuria fava ASU5* crude enzyme displayed biodiesel yield (83.08%) when conducted using optimized reaction conditions of 60 °C, pH ~8, and 1:2 oil/methanol molar ratios. The main goal of the current study is to increase the rate of the transesterification reaction for bacterial lipase purification in order to achieve a high conversion of oily substrates associated with higher biodiesel yield. The immobilization of the bacterial lipases by the nanocomposites may improve the enzyme biocatalyst stability and reusability. Various methods were used for the immobilization of the lipases through adsorption, encapsulation, ionic bonding, cross-linking, and entrapments [35,36], with the goal to enhance the resistance of the lipases to methanol and glycerol inhibitory effect [37,38]. Due to their exceptional physical and chemical properties, magnetic nanoparticles (NPs) have been identified as a class of nanostructured materials of current interest Magnetic Fe_3O_4 NPs have low toxicity [39], large surface area, high mass transfer, and stability under storage and operating conditions [40]. As Fe_3O_4-cellulose nanocomposite possesses a high surface area and a biocompatible environment for the immobilization of enzymes [41]. As a result, many advantages may be obtained from such a system including better functionality and purification [42]; with improved dispersion characteristics and high binding capacity of the biological elements [43]. This is in addition to fewer environmental concerns associated with renewable and biodegradable cellulosic materials; and inhibits the adsorption of non-targeted compounds due to the carbohydrate nature of nanocellulose that may provide a non-stick surface. Interestingly, it was found that lipase enzymes produced by various microbes such as; *Penicillium expansum* [44], *Bacillus* sp. [45], *Candida* sp. 99125 [46] and *Burkholderia* [47] have lower operational costs and higher product purity compared to chemical methods.

3.2. Synthesis and Characterization of Nanocomposite and Immobilization of Kocuria flava ASU5 Lipases

Nowadays, there is a continuous need to improve and expand methods for enzyme immobilization to develop new procedures which are more economic with better performance. Recent explorations focus on the development of novel forms with good characteristics, including better stability, more biocompatibility, and are readily available having a large surface area for higher enzyme immobilization efficiency. Since they may increase reusability and reduce the mass loss of the nano-catalyst throughout the separation processes, magnetic-nanocellulose supports are used in the current work to enhance the separation efficiency of the immobilized enzymes.

The FTIR spectra of Fe_3O_4 NPs showed many function groups and that the stretching and bending vibration of O–H groups of the magnetite surface and adsorbed water can be detected at 3424 cm^{-1} and 1628 cm^{-1}, respectively [48]. The two strong bands at 634 cm^{-1} and 560 cm^{-1} indicate the formation of magnetic nanoparticles [49]. The band located at 560 cm^{-1} can be assigned to the Fe–O stretching vibration of tetrahedral sites of the spinel structure, which confirms the formation of the magnetite phase in the sample [50]. The band that was observed at 445 cm^{-1} may be related to the tetrahedral and the octahedral sites [51]. Moreover, the bands at 2921 cm^{-1} and 2850 cm^{-1} are ascribed to the C-H stretching vibrational of ethanol that is used for washing the precipitate. As well, the FTIR spectra of the nanocellulose, revealed the characteristic bands can be assigned as follows: 3416 cm^{-1} (stretching vibration of O–H group), 2901 cm^{-1} and 1373 cm^{-1} (stretching and deformation vibrations of C–H group in glucose unit), 1640 cm^{-1} (C=O stretching) 1431 cm^{-1} (–CH_2-deformation vibration), 1164 cm^{-1} and 1060 cm^{-1} (C–O stretching mode), 1113 cm^{-1} and 1033 cm^{-1} (C–O–C stretching) and 902 cm^{-1} (β-glycosidic linkage between glucose units). Other characteristic bands for nano-celluolose at 670 and 615 cm^{-1} were related to C–C–O and C–OH groups [52]. The stretching band (1570 cm^{-1}) also indicated the formation of hydrogen bonding between the hydroxyl group of the nanocellulose and the amino group of bacterial lipase [53]. The other characteristic bands of pure nanocellu-

lose were the same as Fe_3O_4/nanocellulose and Fe_3O_4/nanocellulose/lipase enzyme. No characteristic bands of Fe_3O_4 NPs or lipase enzyme could be detected which may be due to their low band intensities or overlapping with that of pure nanocellulose. Xie and Huang found that the IR bands at 1642 cm^{-1} and 1551 cm^{-1}, which are corresponding to amide I and II of the lipase are overlapped with the COO$^-$ anti-symmetric and symmetric stretching vibration of the support [54]. The presence of epoxy groups (C–O–C) acts as multipoint covalent binding sites between the lipase and the Fe_3O_4/nanocellulose composite, therefore reducing the lipase enzyme mobility and enhancing the enzyme's long-term stability [55]. In addition, the presence of carboxyl groups (C=O) is activated by the easily binding of the lipase enzyme forming amide linkage between the Fe_3O_4/nanocellulose composite and the enzyme. The obtained results are in accordance with other already published papers [17,56]. Immobilization of bacterial lipase was achieved by the formation of covalent bonds between bacterial lipase enzyme and Fe_3O_4/cellulose nanocomposite. This approach of immobilization produces stable and recyclable immobilized enzymes when compared with enzyme immobilization via entrapment methods or physical adsorption [57]. Interestingly, Wang et al. [58] and Zhang et al. [59] reported that covalent-immobilized enzyme using cellulose-gold nanocomposites decreases protein unfolding and enables the enzymes to operate as free enzymes without inactivation. Furthermore, the presence of various functional groups capable of covalent binding or activation to give binding sites makes this approach a generally applicable technique of enzyme immobilization [42,60].

From transmission electron microscope images, it was observed that the Fe_3O_4 NPs have a spherical shape (average particle size of ~34.5 nm) and nanocellulose exhibited a fiber structure (average width of ~49 nm and an average length of ~526 nm),whereas the Fe_3O_4/nanocellulose nanocomposite displayed small dark-colored spherical particles and a fiber-like structure. Such characteristics may be attributed to the magnetite Fe_3O_4 and the nanocellulose, respectively. This also confirms that the Fe_3O_4 NPs were successfully composited with the nanocellulose as a support material [32]. Costantini and Califano [33] stated that the immobilization of lipase using nanoparticles is an excellent alternative tactic due to their combination of thermal and mechanical stabilities with regulated textural properties. Additionally, the abundance of surface hydroxyl groups makes it simple to chemically modify surfaces. The last factor is the most crucial as lipases have a strong attraction for hydrophobic supports. Nanocellulose is a biomaterial recovered from acid hydrolysis of native biological cellulosic materials. It was reported that the formation of nanocellulose based on the extraction method, might be rod-shaped, spherical, or have a network shaped with a very high surface area [61]. The unique characteristics of the nanocellulose including large surface area, high surface/volume ratio, high stiffness and strength, and lack of toxicity make nanocellulose an attractive biomaterial used in many industries and functions as drug delivery, protein immobilization, biosensors, medical devices, and nanocomposite applications [60,62–64]. Recently, there has been increased interest in the development of composite materials consisting of more components to achieve more sensitivity and stability for improving their applicability [58,59,65], due to the synergistic characteristics initiated from the components of the mixed nanomaterials. These nanocomposites are more appealing than other composite materials. So, the current study aimed to develop reliable immobilized enzymes with new nanocomposites that can improve their potential in biofuel technology. Combining Fe_3O_4 magnetic nanoparticles with nanocellulose has proven to be an efficient tactic for producing nanocomposite materials capable of immobilizing enzymes and producing a highly active bio-catalytic support suitable for green energy applications [60].

3.3. Characterization of Partially Purified Free Kocuria flava ASU5 Lipase and Immobilized Lipases
3.3.1. Effect of Reaction Temperature

The highest specific activities for the partially purified free lipase activity were 55 °C and the highest lipase activity for the immobilized lipase was 60 °C. At the optimum conditions, the specific activity of the immobilized lipase (36.97 U/mg protein) was higher

than that of the partially purified free lipase (34.05 U/mg protein), then a reduction in the lipase-specific activities was noted. The decline of the lipase-specific activity may be attributed to the slowing down of the enzyme metabolic activity and the denaturation of the bacterial lipase proteins [66]. Priyanka et al. [67] reported that the activity of the *Pseudomonas reinekei* lipases was reduced by 70% at temperatures higher than 50 °C at 1 h. This is in contrast to the lipase activity maintained at about 90% of the initial activity at 40 °C at one day of reaction. Furthermore, *Pseudomonas* sp. AG-8 lipase exhibited optimum activity at a reaction temperature of 45 °C [68].

3.3.2. Effect of Hydrogen Ion Concentration

The highest lipase activity was estimated at the optimum pH value of ~8 and then the enzyme activity declined with increasing the pH value. It was reported that pH plays a significant role in the stability of enzymes by preserving their three-dimensional structure, which is necessary for their biological function [69]. The optimum pH for the lipase enzyme activities is within the alkaline range which may be attributed to the higher affinity of the substrate to the enzyme active catalytic site in the alkaline medium than in the acidic one. Similarly, it was reported that most of the bacterial lipases had an optimum pH in the alkaline range. In specific instances, certain bacterial lipases like those of *Bacillus subtilis* had an optimum activity at high alkaline pH (10–11.5). Talon et al. [70] reported that the optimum pH for *Staphylococcus warneri* lipase enzyme activity was 9 as well as the highest lipase activities for *Staphylococus hyicus* and *Staphylococus haemolyticus* were recorded in alkaline pH [71]. Moreover, the *Pseudomonas* and *Bacillus* lipases were more stable at alkaline pH conditions. Shah and Bhatt [72] stated that *B. subtilis* lipase was more stable with more than 70% activity over a wider pH range of 5–10.

3.3.3. Assay of Thermo-Stability and Immobilized Enzyme Kinetics

The partially purified free lipases retained 90% of their activity for 15 min at 50 °C then a rapid decline with increasing the reaction temperature was observed, whereas the immobilized lipase could retain its high specific activity at 80 °C for 30 min. The high stability of the immobilized lipases at high temperatures may be due to the strong binding of the bacterial lipase and the nanocomposite and consequently, protect the immobilized lipases from unfolding through increasing lipase enzyme rigidity. It was reported that the highest lipase activity of *Bacillus subtilis* (Pa2 lipase) was at temperatures ranging between 30 °C to 50 °C. 70% of its initial activity was indicated at 45 °C. Then lipase activity decreased rapidly at 60 °C [72]. Sztajer et al. [73] reported that the optimum temperature for oil hydrolysis by *Pseudomonas fluorescence* lipase was between 50 and 55 °C. Furthermore, the optimum temperature of lipases produced by mesophilic microorganisms was within the temperature range of 45–60 °C. Interestingly, several thermophilic bacterial strains of *Bacillus* produced thermostable lipases that are active between 60 and 75 °C [74–76]. The kinetics of the immobilized lipase enzyme K_m and V_{max} values were 0.02 mM and 32.47 U/mg protein, respectively. The lowest Km value indicates the highest affinity of the immobilized lipase to the substrate [67].

3.4. The Efficiency for Biodiesel Synthesis and the Reusability of the Immobilized Lipase

Biodiesel yield from waste cooking oils by lipase transesterification process was 91.07% at a reaction temperature of 60 °C and incubation period of 5 h and the highest concentration of fatty acid methyl ester recorded from GC/MS analysis were 9-octadecenoic acid, hexadecanoic acid, octadecanoic acid, heptanoic acid, 9,12-octadecadienoic acid, and 9,10-epoxy-octadecanoic acid methyl esters. The ability to reuse *Kocuria flava* immobilized lipases is crucial, particularly for industrial applications. The immobilized lipase retained its activity after four times assay recording 74.53% fatty acid methyl esters (FAMEs). The active lipase conformational structure alteration during the enzymatic biodiesel synthesis may be the cause of the corresponding decline in the lipase enzymatic activity. Similarly, Xie and Huang [17] stated that the immobilized lipase enzyme could be reused for 5 runs

without any significant loss in its enzymatic activity producing 79.4% biodiesel yield. The determining characteristics of the produced fatty acid methyl esters (biodiesel) in the current study were in the range of both biodiesel standard specification US ASTM D6751 and EU EN 14214. Interestingly, the obtained results of the lipase trans-esterified waste cooking oils were compatible with the results of the waste cooking oil properties and the biodiesel from waste cooking oil [77]. Ramalingam et al. [78] stated that biodiesel production from lipase enzyme is non-toxic, biodegradable biofuel and increases lubricity of diesel fuels, as well as biodiesel being compatible with diesel engines due to the similarity in their physicochemical properties. Consequently, waste cooking oils may be a promising renewable feedstock for biodiesel synthesis; especially since millions of tons of waste cooking oils are generated from several countries all over the world [79–81]. In addition, the application of waste cooking oils as a feedstock for biodiesel production may reduce the production cost of biodiesel by 60–90% [82].

4. Materials and Methods

4.1. Kocuria flava Lipase Enzyme Production

Thermotolerant bacteria *Kocuria flava*, isolated from cooking oil waste, was grown in a liquid medium containing (g/L): peptone, 15; yeast extract, 5; NaCl, 2; $MgSO_4$, 0.4; KH_2PO_4, 0.3; K_2HPO_4, 0.3; in addition to 10 mL of filtrated used cooking oil waste which is used as a substrate for lipase induction. To isolate the lipase enzyme from the bacterial cells, the above culture was centrifuged at 8000 rpm for 10 min. The supernatant was collected for lipase purification by ammonium sulfate saturation process followed by dialysis of the dissolved precipitate in Tris- HCl buffer solution, pH 7.8. Then the enzyme activity assay was determined according to Tripathi et al. [83], and the protein content was assayed according to Lowry et al. [84]. The partially purified enzyme was kept in a deep freezer at −80 °C for enzyme immobilization.

4.2. Preparation of Nanocomposite

4.2.1. Materials

All chemicals were used in their original status and did not undergo any further purification. Ferric chloride hexahydrate ($FeCl_3.6H_2O$), ammonium ferrous sulfate hexahydrate (($NH_4)_2Fe(SO_4)_2.6H_2O$), and sodium hydroxide (NaOH) were purchased from Alpha chemicals (Cairo, Egypt).

4.2.2. Synthesis of Fe_3O_4 Nanoparticles (NPs)

Fe_3O_4 NPs were synthesized as described by the co-precipitation method. Typically, 35 g of $FeCl_3.6H_2O$ and 25.4 g of ($NH_4)_2Fe(SO_4)_2.6H_2O$ were dissolved in 300 mL of bi-distilled water. Then, a mixture of iron salts was added dropwise into 500 mL (2.5 M) of NaOH solution with vigorous stirring to ensure good mixing. After that, the reaction mixture was heated at 60 °C with constant stirring for 2 h. At 2 h, the mixture was left at room temperature to cool down. The formed black precipitate was separated by an external magnet and washed several times with bi-distilled water and ethanol. The collected precipitate was, then, dried in an oven at 60 °C overnight, the obtained powder was Fe_3O_4, and was stored for further use.

4.2.3. Preparation of Cellulosic Nanomaterials from Waste Papers

Nanocellulose was conducted by the acid hydrolysis process as follows: 1 g of the pretreated wastepaper was mixed with 100 mL sulfuric acid 65% at 60 °C for 1 h. The produced suspension was centrifuged at 6000 rpm for 15 min and the precipitate was washed with distilled water until neutral pH was achieved. The produced nanocellulose was characterized by FTIR (Thermo Scientific Nicolet iS10 FT-IR Spectrometer, Madison, USA) and Transmission electron microscope (JEOL TEM, Model 100 CX II; Tokyo, Japan) analysis.

4.2.4. Preparation of Fe₃O₄ Magnetic-Cellulosic Nanocomposites

0.1 g Fe₃O₄ NPs were suspended in 60 mL acetonitrile, then 0.4 g of nanocellulose was added to the mixture. The resulting mixture was then macerated for 20 min. Subsequently, the produced magnetic nanocomposite was collected, washed with ethyl alcohol, and dried at 60 °C for 24 h.

4.3. Immobilization of Lipase Enzyme with Fe₃O₄ Magnetic-Cellulosic Nanocomposites

Firstly, 0.1g Fe₃O₄-cellulose nanocomposite was dispersed in 100 mL distilled water, then the mixture was continuously stirred at 25 °C for 2 h. After that, the nanocomposite was recovered and washed with distilled water. For lipase immobilization, a *Kocuria flava* lipase was dissolved in a phosphate buffer solution (100 mM, pH 7). After this, the Fe₃O₄-cellulose nanocomposite was dipped in the *Kocuria flava* lipase buffer solution and incubated for 5 h at 30 °C in a shaking water bath. Subsequently, the lipase-immobilized material was collected by the magnetic field, then washed with phosphate buffer, and finally frozen overnight and kept at −80 °C for further uses. The lipase enzyme immobilization efficacy was estimated according to the following equation [17]:

$$q = \left(C_i - C_f \right) V_1 / C_i V_2 (\%) \tag{1}$$

where q is the enzyme immobilization efficacy (%), C_i and C_f are the initial and final protein concentrations (in mg mL^{-1}) in the immobilization solution, respectively; V_1 and V_2 are the initial and final volume of the solution (mL), respectively.

4.4. Optimization and Characterization of the Lipase Enzyme Activity

The effect of different reaction temperatures (15, 20, 25, 30, 35, 40, and 45 °C) and different pH values using different buffers including: citrate phosphate buffer (pH 3–7), sodium phosphate buffer (pH 7–8) and glycine-NaOH buffer (pH 9–10) were used to evaluate the lipase specific activities of the partially purified free enzyme and immobilized lipases. In addition, the lipase thermo-stability at different temperatures (50–90 °C) was determined at different time intervals. The lipase enzyme activity of partially purified free and immobilized lipase of *Kocuria flava* ASU5 (MT919305) was assayed as described by Najjar et al. [34]. All the experiments were performed in triplicates.

4.5. Kinetics of Immobilized Enzyme Reusability

The Michaelis-Menten constant (K_m) and maximum velocity (V_{max}) value of the immobilized lipase enzyme was assessed at different *para*-nitro phenyl-palmitate concentrations under the optimum assay conditions using Lineweaver-Burk plots (double reciprocal plot) that describe enzyme kinetics [85]. In this plot, the reaction rate inverse ($1/V$) was plotted against the substrate concentration inverse ($1/S$). The Lineweaver-Burk plot is represented by a straight line in which

$$The\ slope = K_M / V_{max} \tag{2}$$

$$Y\ intercept = 1 / V_{max} \tag{3}$$

4.6. Assay for Immobilized Enzyme Reusability

The immobilized enzyme was assayed for its reusability and recyclability in the transesterification process several times under optimum reaction conditions. To estimate the stability of the immobilized lipase of *Kocuria flava* ASU5, a multi-cyclic assay using the Fe₃O₄/cellulose nanocomposite biocatalyst was performed by adding fresh cooking oil wastes. The biocatalyst was collected then rinsed out with phosphate buffer (100 mM, pH 7), and finally frozen down for further use in a new transesterification reaction.

4.7. Biodiesel Production from Waste Oil by Immobilized Lipase Enzyme

Biodiesel synthesis from cooking oil wastes was performed using the immobilized lipase as a biocatalyst using 5 mL stopper glass vials as described by Najjar et al. [34].

The biodiesel yield (% FAME) from the transesterification process was measured using GC/MS (Thermo Scientific, Model: DPC-Direct Probe Controller (DPC-20451), USA, Austin, TX78728) at the Chemistry Department, Faculty of Science, Assiut University [34].

4.8. Determination of the Physicochemical Characteristics

The characteristics [density (ρ), kinematic viscosity (ν_{mix}), iodine value (IV), saponification number (SN), higher heating value (HHV), and Cetane Number (CN), free fatty acid (FFA)] of the produced biodiesel was estimated based on the mathematical equations [86–92]:

$$\rho = \sum(c_i \rho_i) \tag{4}$$

$$\nu_{mix} = \sum(A_c x v_c) \tag{5}$$

$$SN = \sum(254 \times A_i) / MW_i \tag{6}$$

$$IV = \sum(254 \times \text{D} \times A_i) / MW_i \tag{7}$$

$$HHV = 49.43 - [0.041(SN) + 0.015(IV)] \tag{8}$$

$$CN = 1.068 \sum(CN_i W_i) - 6.747 \tag{9}$$

These characteristics were compared with the standard biodiesel "US biodiesel standard specification ASTM D6751 and EU biodiesel standard EN 14214.

Where,

c_i = the concentration (mass fraction)

ρ_i = the density of component (individual the fatty acid methyl ester) present in the biodiesel

ν_{mix} = the kinematic viscosity of the biodiesel sample (the mixture of fatty acid alkyl esters),

A_c = the relative amount (%/100) of the individual neat ester in the mixture (as determined by, GC/Ms)

ν_c = obtained from the kinematic viscosity database of the individual FAME present in biodiesel

A_i = the percentage,

D = the number of the double bonds

MW_i = the molecular mass of each fatty acid methyl ester

CN_i = reported CN of pure fatty acid methyl esters available in the database

W_i = the mass fraction of the individual fatty ester components detected and quantified by GC/MS.

5. Conclusions

The development of magnetic Fe_3O_4-cellulose nanocomposites for the immobilization of *Kocuria flava* ASU5 lipase may provide a prospective novel recyclable *Kocuria flava* immobilized lipase for transesterification of waste cooking oils for biodiesel production. The findings of this work clearly demonstrate that Fe_3O_4-cellulose nanocomposite showed much superior stability towards pH, thermal, and methanol denaturation as well as good recyclable properties following hydrolysis of the used cooking oil. Together, these findings showed the nanocomposite's potential for use in the immobilization of the lipase enzyme. Moreover, the application of magnetic Fe_3O_4-nanocellulose/lipase and the recovery of the biocatalyst may increase the feasibility of the downstream process by magnetic separation without extensive enzymatic activity loss. The immobilized lipase can be reutilized for up to four cycles maintaining about 70% of the initial enzyme activity. As a result, using this biocatalyst may be more advantageous from an economic and environmental standpoint, and research indicates that it has a great deal of potential for use as a reliable biocatalyst to produce biodiesel. Although there are advantages presented by this method, there are limitations also, such as the high costs of enzyme purification especially highly purified enzymes, poor stability, and the enzyme deactivation by successive subjection to alcohol and partly by the generated glycerol.

References

1. Goldemberg, J. Ethanol for a Sustainable Energy Future. *Science* **2007**, *315*, 808–810. [CrossRef] [PubMed]
2. Uddin, W. *Mobile and Area Sources of Greenhouse Gases and Abatement Strategies BT—Handbook of Climate Change Mitigation and Adaptation*; Lackner, M., Sajjadi, B., Chen, W.-Y., Eds.; Springer International Publishing: Cham, Switzerland, 2022; pp. 743–807, ISBN 978-3-030-72579-2.
3. Hawkes, F.R.; Dinsdale, R.; Hawkes, D.L.; Hussy, I. Sustainable Fermentative Hydrogen Production: Challenges for Process Optimisation. *Int. J. Hydrogen Energy* **2002**, *27*, 1339–1347. [CrossRef]
4. Afolalu, S.A.; Yusuf, O.O.; Abioye, A.A.; Emetere, M.E.; Ongbali, S.O.; Samuel, O.D. Biofuel; A Sustainable Renewable Source Of Energy-A Review. *IOP Conf. Ser. Earth Environ. Sci.* **2021**, *665*, 12040. [CrossRef]
5. Hassan, E.A.; Abd-Alla, M.H.; Bagy, M.M.K.; Morsy, F.M. In Situ Hydrogen, Acetone, Butanol, Ethanol and Microdiesel Production by *Clostridium acetobutylicum* ATCC 824 from Oleaginous Fungal Biomass. *Anaerobe* **2015**, *34*, 125–131. [CrossRef]
6. Califano, V.; Bloisi, F.; Perretta, G.; Aronne, A.; Ausanio, G.; Costantini, A.; Vicari, L. Frozen Microemulsions for MAPLE Immobilization of Lipase. *Molecules* **2017**, *22*, 2153. [CrossRef]
7. Meher, L.C.; Vidya Sagar, D.; Naik, S.N. Technical Aspects of Biodiesel Production by Transesterification—A Review. *Renew. Sustain. Energy Rev.* **2006**, *10*, 248–268. [CrossRef]
8. Amini, Z.; Ilham, Z.; Ong, H.C.; Mazaheri, H.; Chen, W.-H. State of the Art and Prospective of Lipase-Catalyzed Transesterification Reaction for Biodiesel Production. *Energy Convers. Manag.* **2017**, *141*, 339–353. [CrossRef]
9. Sankaran, R.; Show, P.L.; Chang, J.-S. Biodiesel Production Using Immobilized Lipase: Feasibility and Challenges. *Biofuels Bioprod. Biorefin.* **2016**, *10*, 896–916. [CrossRef]
10. Xie, W.; Huang, M. Immobilization of Candida Rugosa Lipase onto Graphene Oxide Fe₃O₄ Nanocomposite: Characterization and Application for Biodiesel Production. *Energy Convers. Manag.* **2018**, *159*, 42–53. [CrossRef]
11. Dhawane, S.H.; Chowdhury, S.; Halder, G. Lipase Immobilised Carbonaceous Catalyst Assisted Enzymatic Transesterification of *Mesua ferrea* Oil. *Energy Convers. Manag.* **2019**, *184*, 671–680. [CrossRef]
12. Cipolatti, E.P.; Valério, A.; Henriques, R.O.; Moritz, D.E.; Ninow, J.L.; Freire, D.M.G.; Manoel, E.A.; Fernandez-Lafuente, R.; de Oliveira, D. Nanomaterials for Biocatalyst Immobilization—State of the Art and Future Trends. *RSC Adv.* **2016**, *6*, 104675–104692. [CrossRef]
13. Garcia-Galan, C.; Berenguer-Murcia, Á.; Fernandez-Lafuente, R.; Rodrigues, R.C. Potential of Different Enzyme Immobilization Strategies to Improve Enzyme Performance. *Adv. Synth. Catal.* **2011**, *353*, 2885–2904. [CrossRef]
14. Xie, W.; Zang, X. Lipase Immobilized on Ionic Liquid-Functionalized Magnetic Silica Composites as a Magnetic Biocatalyst for Production of Trans-Free Plastic Fats. *Food Chem.* **2018**, *257*, 15–22. [CrossRef]
15. Khoshnevisan, K.; Bordbar, A.-K.; Zare, D.; Davoodi, D.; Noruzi, M.; Barkhi, M.; Tabatabaei, M. Immobilization of Cellulase Enzyme on Superparamagnetic Nanoparticles and Determination of Its Activity and Stability. *Chem. Eng. J.* **2011**, *171*, 669–673. [CrossRef]
16. Xie, W.; Zang, X. Covalent Immobilization of Lipase onto Aminopropyl-Functionalized Hydroxyapatite-Encapsulated-γ-Fe₂O₃ Nanoparticles: A Magnetic Biocatalyst for Interesterification of Soybean Oil. *Food Chem.* **2017**, *227*, 397–403. [CrossRef] [PubMed]
17. Xie, W.; Huang, M. Fabrication of Immobilized *Candida rugosa* Lipase on Magnetic Fe₃O₄-Poly(Glycidyl Methacrylate-Co-Methacrylic Acid) Composite as an Efficient and Recyclable Biocatalyst for Enzymatic Production of Biodiesel. *Renew. Energy* **2020**, *158*, 474–486. [CrossRef]
18. Ren, Y.; Rivera, J.G.; He, L.; Kulkarni, H.; Lee, D.-K.; Messersmith, P.B. Facile, High Efficiency Immobilization of Lipase Enzyme on Magnetic Iron Oxide Nanoparticles via a Biomimetic Coating. *BMC Biotechnol.* **2011**, *11*, 63. [CrossRef]

19. Karimi, M. Immobilization of Lipase onto Mesoporous Magnetic Nanoparticles for Enzymatic Synthesis of Biodiesel. *Biocatal. Agric. Biotechnol.* **2016**, *8*, 182–188. [CrossRef]

20. Xie, W.; Wang, J. Enzymatic Production of Biodiesel from Soybean Oil by Using Immobilized Lipase on Fe_3O_4/Poly(Styrene-Methacrylic Acid) Magnetic Microsphere as a Biocatalyst. *Energy Fuels* **2014**, *28*, 2624–2631. [CrossRef]

21. Qiao, J.; Wang, T.; Zheng, K.; Zhou, E.; Shen, C.; Jia, A.; Zhang, Q. Magnetically Reusable Fe_3O_4@NC@Pt Catalyst for Selective Reduction of Nitroarenes. *Catalysts* **2021**, *11*, 1219. [CrossRef]

22. Polshettiwar, V.; Varma, R.S. Green Chemistry by Nano-Catalysis. *Green Chem.* **2010**, *12*, 743–754. [CrossRef]

23. Xia, H.; Cui, B.; Zhou, J.; Zhang, L.; Zhang, J.; Guo, X.; Guo, H. Synthesis and Characterization of Fe_3O_4@C@Ag Nanocomposites and Their Antibacterial Performance. *Appl. Surf. Sci.* **2011**, *257*, 9397–9402. [CrossRef]

24. Nasrollahzadeh, M.; Mohammad Sajadi, S.; Rostami-Vartooni, A.; Khalaj, M. Green Synthesis of Pd/Fe_3O_4 Nanoparticles Using Euphorbia Condylocarpa M. Bieb Root Extract and Their Catalytic Applications as Magnetically Recoverable and Stable Recyclable Catalysts for the Phosphine-Free Sonogashira and Suzuki Coupling Reactions. *J. Mol. Catal. A Chem.* **2015**, *396*, 31–39. [CrossRef]

25. Atarod, M.; Nasrollahzadeh, M.; Sajadi, S.M. Green Synthesis of a Cu/Reduced Graphene Oxide/Fe_3O_4 Nanocomposite Using *Euphorbia wallichii* Leaf Extract and Its Application as a Recyclable and Heterogeneous Catalyst for the Reduction of 4-Nitrophenol and Rhodamine B. *RSC Adv.* **2015**, *5*, 91532–91543. [CrossRef]

26. Ghazanfari, M.R.; Kashefi, M.; Shams, S.F.; Jaafari, M.R. Perspective of Fe_3O_4 Nanoparticles Role in Biomedical Applications. *Biochem. Res. Int.* **2016**, *2016*, 7840161. [CrossRef]

27. Ullah, K.; Ahmad, M.; Sultana, S.; Teong, L.K.; Sharma, V.K.; Abdullah, A.Z.; Zafar, M.; Ullah, Z. Experimental Analysis of Di-Functional Magnetic Oxide Catalyst and Its Performance in the Hemp Plant Biodiesel Production. *Appl. Energy* **2014**, *113*, 660–669. [CrossRef]

28. Zhang, F.; Fang, Z.; Wang, Y.-T. Biodiesel Production Directly from Oils with High Acid Value by Magnetic Na_2SiO_3@Fe_3O_4/C Catalyst and Ultrasound. *Fuel* **2015**, *150*, 370–377. [CrossRef]

29. Serga, V.; Burve, R.; Maiorov, M.; Krumina, A.; Skaudžius, R.; Zarkov, A.; Kareiva, A.; Popov, A.I. Impact of Gadolinium on the Structure and Magnetic Properties of Nanocrystalline Powders of Iron Oxides Produced by the Extraction-Pyrolytic Method. *Materials* **2020**, *13*, 4147. [CrossRef]

30. Li, Y.; Wang, Z.; Liu, R. Superparamagnetic α-Fe_2O_3/Fe_3O_4 Heterogeneous Nanoparticles with Enhanced Biocompatibility. *Nanomaterials* **2021**, *11*, 834. [CrossRef]

31. Niculescu, A.-G.; Chircov, C.; Grumezescu, A.M. Magnetite Nanoparticles: Synthesis Methods—A Comparative Review. *Methods* **2022**, *199*, 16–27. [CrossRef]

32. Helmiyati, H.; Anggraini, Y. Nanocomposites Comprising Cellulose and Nanomagnetite as Heterogeneous Catalysts for the Synthesis of Biodiesel from Oleic Acid. *Int. J. Technol.* **2019**, *10*, 798. [CrossRef]

33. Costantini, A.; Califano, V. Lipase Immobilization in Mesoporous Silica Nanoparticles for Biofuel Production. *Catalysts* **2021**, *11*, 629. [CrossRef]

34. Najjar, A.; Hassan, E.; Zabermawi, N.; Hassan, S.; Bajrai, L.; Almuhayawi, M.; Abujamel, T.; Almasaudi, S.; Azhar, L.; Moulay, M.; et al. Optimizing the Catalytic Activities of Methanol and Thermotolerant *Kocuria flava* Lipases for Biodiesel Production from Cooking Oil Wastes. *Sci. Rep.* **2021**, *11*, 13659. [CrossRef] [PubMed]

35. Garlapati, V.K.; Kant, R.; Kumari, A.; Mahapatra, P.; Das, P.; Banerjee, R. Lipase Mediated Transesterification of *Simarouba glauca* Oil: A New Feedstock for Biodiesel Production. *Sustain. Chem. Process.* **2013**, *1*, 11. [CrossRef]

36. Islam, A.; Taufiq-Yap, Y.H.; Chan, E.-S.; Moniruzzaman, M.; Islam, S.; Nabi, M.N. Advances in Solid-Catalytic and Non-Catalytic Technologies for Biodiesel Production. *Energy Convers. Manag.* **2014**, *88*, 1200–1218. [CrossRef]

37. Gog, A.; Roman, M.; Toşa, M.; Paizs, C.; Irimie, F.D. Biodiesel Production Using Enzymatic Transesterification—Current State and Perspectives. *Renew. Energy* **2012**, *39*, 10–16. [CrossRef]

38. Macario, A.; Moliner, M.; Diaz, U.; Jorda, J.L.; Corma, A.; Giordano, G. Biodiesel Production by Immobilized Lipase on Zeolites and Related Materials. In *Zeolites and Related Materials: Trends, Targets and Challenges*; Gédéon, A., Massiani, P., Babonneau, F., Eds.; Elsevier: Amsterdam, The Netherlands, 2008; Volume 174, pp. 1011–1016, ISBN 0167-2991.

39. Gupta, A.K.; Gupta, M. Synthesis and Surface Engineering of Iron Oxide Nanoparticles for Biomedical Applications. *Biomaterials* **2005**, *26*, 3995–4021. [CrossRef]

40. Sheldon, R.A. Enzyme Immobilization: The Quest for Optimum Performance. *Adv. Synth. Catal.* **2007**, *349*, 1289–1307. [CrossRef]

41. Daniel, M.-C.; Astruc, D. Gold Nanoparticles: Assembly, Supramolecular Chemistry, Quantum-Size-Related Properties, and Applications toward Biology, Catalysis, and Nanotechnology. *Chem. Rev.* **2004**, *104*, 293–346. [CrossRef]

42. Jung, U.-Y.; Park, J.-W.; Han, E.-H.; Kang, S.-G.; Lee, S.; Jun, C.-H. Facile One-Step Catalytic Grafting of N-Hydroxysuccinimidyl-Ester-Functionalized Methallylsilane onto Silica for Enzyme Immobilization. *Chem.—Asian J.* **2011**, *6*, 638–645. [CrossRef]

43. Tsai, T.-W.; Heckert, G.; Neves, L.F.; Tan, Y.; Kao, D.-Y.; Harrison, R.G.; Resasco, D.E.; Schmidtke, D.W. Adsorption of Glucose Oxidase onto Single-Walled Carbon Nanotubes and Its Application in Layer-By-Layer Biosensors. *Anal. Chem.* **2009**, *81*, 7917–7925. [CrossRef] [PubMed]

44. Lai, J.-Q.; Hu, Z.-L.; Sheldon, R.A.; Yang, Z. Catalytic Performance of Cross-Linked Enzyme Aggregates of *Penicillium expansum* Lipase and Their Use as Catalyst for Biodiesel Production. *Process Biochem.* **2012**, *47*, 2058–2063. [CrossRef]

45. Sivaramakrishnan, R.; Muthukumar, K. Isolation of Thermo-Stable and Solvent-Tolerant *Bacillus* sp. Lipase for the Production of Biodiesel. *Appl. Biochem. Biotechnol.* **2012**, *166*, 1095–1111. [CrossRef]

46. Li, Z.; Yuan, H.; Yang, J.; Li, B. Optimization of the Biomass Production of Oil Algae *Chlorella minutissima* UTEX2341. *Bioresour. Technol.* **2011**, *102*, 9128–9134. [CrossRef] [PubMed]

47. Tran, D.-T.; Chen, C.-L.; Chang, J.-S. Effect of Solvents and Oil Content on Direct Transesterification of Wet Oil-Bearing Microalgal Biomass of *Chlorella vulgaris* ESP-31 for Biodiesel Synthesis Using Immobilized Lipase as the Biocatalyst. *Bioresour. Technol.* **2013**, *135*, 213–221. [CrossRef]

48. Zavareh, S.; Behrouzi, Z.; Avanes, A. Cu (II) Binded Chitosan/Fe$_3$O$_4$ Nanocomomposite as a New Biosorbent for Efficient and Selective Removal of Phosphate. *Int. J. Biol. Macromol.* **2017**, *101*, 40–50. [CrossRef]

49. Wei, Y.; Han, B.; Hu, X.; Lin, Y.; Wang, X.; Deng, X. Synthesis of Fe$_3$O$_4$ Nanoparticles and Their Magnetic Properties. *Procedia Eng.* **2012**, *27*, 632–637. [CrossRef]

50. Pham, X.N.; Nguyen, T.P.; Pham, T.N.; Tran, T.T.N.; Tran, T.V.T. Synthesis and Characterization of Chitosan-Coated Magnetite Nanoparticles and Their Application in Curcumin Drug Delivery. *Adv. Nat. Sci. Nanosci. Nanotechnol.* **2016**, *7*, 45010. [CrossRef]

51. Pati, S.S.; Mahendran, V.; Philip, J. A Simple Approach to Produce Stable Ferrofluids without Surfactants and with High Temperature Stability. *J. Nanofluids* **2013**, *2*, 94–103. [CrossRef]

52. Leung, A.C.W.; Hrapovic, S.; Lam, E.; Liu, Y.; Male, K.B.; Mahmoud, K.A.; Luong, J.H.T. Characteristics and Properties of Carboxylated Cellulose Nanocrystals Prepared from a Novel One-Step Procedure. *Small* **2011**, *7*, 302–305. [CrossRef]

53. Şengül, G.; Demirci, S.; Caykara, T. Preparation, Characterization, and Surface Energetics of Hydroxypropyl Cellulose/Polyethylenimine Blends. *J. Appl. Polym. Sci.* **2009**, *114*, 2751–2754. [CrossRef]

54. Xie, W.; Huang, M. Enzymatic Production of Biodiesel Using Immobilized Lipase on Core-Shell Structured Fe$_3$O$_4$@MIL-100(Fe) Composites. *Catalys* **2019**, *9*, 850. [CrossRef]

55. Zhang, D.-H.; Peng, L.-J.; Wang, Y.; Li, Y.-Q. Lipase Immobilization on Epoxy-Activated Poly(Vinyl Acetate-Acrylamide) Microspheres. *Colloids Surf. B Biointerfaces* **2015**, *129*, 206–210. [CrossRef]

56. Kim, H.; Namgung, R.; Singha, K.; Oh, I.-K.; Kim, W.J. Graphene Oxide–Polyethylenimine Nanoconstruct as a Gene Delivery Vector and Bioimaging Tool. *Bioconjug. Chem.* **2011**, *22*, 2558–2567. [CrossRef] [PubMed]

57. Tischer, W.; Wedekind, F. *Immobilized Enzymes: Methods and Applications*; Fessner, W.-D., Archelas, A., Demirjian, D.C., Furstoss, R., Griengl, H., Jaeger, K.-E., Morís-Varas, E., Öhrlein, R., Reetz, M.T., Reymond, J.-L., et al., Eds.; Springer: Berlin/Heidelberg, Germany, 1999; pp. 95–126, ISBN 978-3-540-68116-8.

58. Wang, W.; Li, H.-Y.; Zhang, D.-W.; Jiang, J.; Cui, Y.-R.; Qiu, S.; Zhou, Y.-L.; Zhang, X.-X. Fabrication of Bienzymatic Glucose Biosensor Based on Novel Gold Nanoparticles-Bacteria Cellulose Nanofibers Nanocomposite. *Electroanalysis* **2010**, *22*, 2543–2550. [CrossRef]

59. Zhang, T.; Wang, W.; Zhang, D.; Zhang, X.; Ma, Y.; Zhou, Y.; Qi, L. Biotemplated Synthesis of Gold Nanoparticle–Bacteria Cellulose Nanofiber Nanocomposites and Their Application in Biosensing. *Adv. Funct. Mater.* **2010**, *20*, 1152–1160. [CrossRef]

60. Mahmoud, K.A.; Male, K.B.; Hrapovic, S.; Luong, J.H.T. Cellulose Nanocrystal/Gold Nanoparticle Composite as a Matrix for Enzyme Immobilization. *ACS Appl. Mater. Interfaces* **2009**, *1*, 1383–1386. [CrossRef] [PubMed]

61. Lu, P.; Hsieh, Y.-L. Preparation and Properties of Cellulose Nanocrystals: Rods, Spheres, and Network. *Carbohydr. Polym.* **2010**, *82*, 329–336. [CrossRef]

62. Jackson, J.K.; Letchford, K.; Wasserman, B.Z.; Ye, L.; Hamad, W.Y.; Burt, H.M. The Use of Nanocrystalline Cellulose for the Binding and Controlled Release of Drugs. *Int. J. Nanomed.* **2011**, *6*, 321–330. [CrossRef]

63. Arola, S.; Tammelin, T.; Setälä, H.; Tullila, A.; Linder, M.B. Immobilization–Stabilization of Proteins on Nanofibrillated Cellulose Derivatives and Their Bioactive Film Formation. *Biomacromolecules* **2012**, *13*, 594–603. [CrossRef]

64. Orelma, H.; Teerinen, T.; Johansson, L.-S.; Holappa, S.; Laine, J. CMC-Modified Cellulose Biointerface for Antibody Conjugation. *Biomacromolecules* **2012**, *13*, 1051–1058. [CrossRef] [PubMed]

65. Hu, X.; Wang, T.; Qu, X.; Dong, S. In Situ Synthesis and Characterization of Multiwalled Carbon Nanotube/Au Nanoparticle Composite Materials. *J. Phys. Chem. B* **2006**, *110*, 853–857. [CrossRef] [PubMed]

66. Sooch, B.; Kauldhar, B. Influence of Multiple Bioprocess Parameters on Production of Lipase from *Pseudomonas* sp. BWS-5. *Braz. Arch. Biol. Technol.* **2013**, *56*, 711–721. [CrossRef]

67. Priyanka, P.; Kinsella, G.; Henehan, G.T.; Ryan, B.J. Isolation, Purification and Characterization of a Novel Solvent Stable Lipase from *Pseudomonas reinekei. Protein Expr. Purif.* **2019**, *153*, 121–130. [CrossRef] [PubMed]

68. Sharma, A.K.; Tiwari, R.P.; Hoondal, G.S. Properties of a Thermostable and Solvent Stable Extracellular Lipase from a *Pseudomonas* sp. AG-8. *J. Basic Microbiol.* **2001**, *41*, 363–366. [CrossRef]

69. Talley, K.; Alexov, E. On the PH-Optimum of Activity and Stability of Proteins. *Proteins Struct. Funct. Bioinform.* **2010**, *78*, 2699–2706. [CrossRef]

70. Talòn, R.; Dublet, N.; Montel, M.-C.; Cantonnet, M. Purification and Characterization of Extracellular *Staphylococcus warneri* Lipase. *Curr. Microbiol.* **1995**, *30*, 11–16. [CrossRef]

71. Rosenstein, R.; Götz, F. Staphylococcal Lipases: Biochemical and Molecular Characterization. *Biochimie* **2000**, *82*, 1005–1014. [CrossRef]

72. Shah, K. Purification and Characterization of Lipase from *B. subtilis* Pa2. *J. Biochem. Technol.* **2012**, *3*, 292–295.

73. Sztajer, H.; Borkowski, J.; Sobiech, K. Purification and Some Properties of *Pseudomonas fluorescens* Lipase. *Biotechnol. Appl. Biochem.* **1991**, *13*, 65–71. [CrossRef]

74. Yasar, G.; Gulhan, U.G.; Guduk, E.; Aktas, F. Screening, Partial Purification and Characterization of the Hyper-Thermophilic Lipase Produced by a New Isolate of *Bacillus subtilis* LP2. *Biocatal. Biotransform.* **2020**, *38*, 367–375. [CrossRef]

75. Abol-Fotouh, D.; AlHagar, O.E.A.; Hassan, M.A. Optimization, Purification, and Biochemical Characterization of Thermoalkaliphilic Lipase from a Novel *Geobacillus stearothermophilus* FMR12 for Detergent Formulations. *Int. J. Biol. Macromol.* **2021**, *181*, 125–135. [CrossRef] [PubMed]

76. Baral, A.; Fox, P.F. Isolation and Characterization of an Extracellular Lipase from *Pseudomonas tolaasii*. *Food Chem.* **1997**, *58*, 33–38. [CrossRef]

77. Demirbas, A. Biodiesel Production from Vegetable Oils via Catalytic and Non-Catalytic Supercritical Methanol Transesterification Methods. *Prog. Energy Combust. Sci.* **2005**, *31*, 466–487. [CrossRef]

78. Ramalingam, S.; Sudagar, S.; Balamurugan, R.; Naveen, R. Performance and Emission Behavior of Biofuel from Milk Scum: A Waste Product from Dairy Industry. *Energy Sources Part A Recover. Util. Environ. Eff.* **2021**, *43*, 968–976. [CrossRef]

79. Balat, M. Potential Alternatives to Edible Oils for Biodiesel Production—A Review of Current Work. *Energy Convers. Manag.* **2011**, *52*, 1479–1492. [CrossRef]

80. Diya'uddeen, B.H.; Abdul Aziz, A.R.; Daud, W.M.A.W.; Chakrabarti, M.H. Performance Evaluation of Biodiesel from Used Domestic Waste Oils: A Review. *Process Saf. Environ. Prot.* **2012**, *90*, 164–179. [CrossRef]

81. Selvaraj, R.; Praveenkumar, R.; Moorthy, I.G. A Comprehensive Review of Biodiesel Production Methods from Various Feedstocks. *Biofuels* **2019**, *10*, 325–333. [CrossRef]

82. Yaakob, Z.; Mohammad, M.; Alherbawi, M.; Alam, Z.; Sopian, K. Overview of the Production of Biodiesel from Waste Cooking Oil. *Renew. Sustain. Energy Rev.* **2013**, *18*, 184–193. [CrossRef]

83. Tripathi, R.; Singh, J.; Bharti, R.K.; Thakur, I.S. Isolation, Purification and Characterization of Lipase from *Microbacterium* sp. and Its Application in Biodiesel Production. *Energy Procedia* **2014**, *54*, 518–529. [CrossRef]

84. Lowry, O.H.; Rosebrough, N.J.; Farr, A.L.; Randall, R.J. Protein Measurement with the Folin Phenol Reagent. *J. Biol. Chem.* **1951**, *193*, 265–275. [CrossRef]

85. Ault, A. An Introduction to Enzyme Kinetics. *J. Chem. Educ.* **1974**, *51*, 381. [CrossRef]

86. Pratas, M.J.; Freitas, S.V.D.; Oliveira, M.B.; Monteiro, S.C.; Lima, Á.S.; Coutinho, J.A.P. Biodiesel Density: Experimental Measurements and Prediction Models. *Energy Fuels* **2011**, *25*, 2333–2340. [CrossRef]

87. Lapuerta, M.; Rodríguez-Fernández, J.; Armas, O. Correlation for the Estimation of the Density of Fatty Acid Esters Fuels and Its Implications. A Proposed Biodiesel Cetane Index. *Chem. Phys. Lipids* **2010**, *163*, 720–727. [CrossRef]

88. Knothe, G.; Steidley, K.R. Kinematic Viscosity of Fatty Acid Methyl Esters: Prediction, Calculated Viscosity Contribution of Esters with Unavailable Data, and Carbon–Oxygen Equivalents. *Fuel* **2011**, *90*, 3217–3224. [CrossRef]

89. Mohibbe Azam, M.; Waris, A.; Nahar, N.M. Prospects and Potential of Fatty Acid Methyl Esters of Some Non-Traditional Seed Oils for Use as Biodiesel in India. *Biomass Bioenergy* **2005**, *29*, 293–302. [CrossRef]

90. Gunstone, F.D.; Harwood, J.L.; Dijkstra, A.J. *The Lipid Handbook with CD-ROM*, 3rd ed.; CRC/Taylor & Francis: Boca Raton, FL, USA, 2007; ISBN 9781420009675.

91. Demirbaş, A. Fuel Properties and Calculation of Higher Heating Values of Vegetable Oils. *Fuel* **1998**, *77*, 1117–1120. [CrossRef]

92. Tong, D.; Hu, C.; Jiang, K.; Li, Y. Cetane Number Prediction of Biodiesel from the Composition of the Fatty Acid Methyl Esters. *J. Am. Oil Chem. Soc.* **2011**, *88*, 415–423. [CrossRef]